INVESTIGATIONS OF ALFVÉN EIGENMODE STABILITY VIA ACTIVE ANTENNA EXCITATION IN JET HYDROGEN, DEUTERIUM, TRITIUM, DT, AND HELIUM PLASMAS

R.A. TINGUELY, M. PORKOLAB
Plasma Science and Fusion Center, Massachusetts Institute of Technology
Cambridge, USA
Email: tinguely@psfc.mit.edu

S. DOWSON
Culham Centre for Fusion Energy, Culham Science Centre
Abingdon, UK

A. FASOLI
Ecole Polytechnique Fédérale de Lausanne (EPFL), Swiss Plasma Center (SPC)
Lausanne, Switzerland

P.G. PUGLIA, J. GARCIA
CEA Institute for Magnetic Fusion Research
Saint-Paul-lez-Durance, France

J. GONZALEZ-MARTIN
University of Seville
Seville, Spain

Y.O. KAZAKOV
Laboratory for Plasma Physics, LPP-ERM/KMS
Brussels, Belgium

M. PODESTÀ
Princeton Plasma Physics Laboratory
Princeton, USA

and JET CONTRIBUTORS[1]

Abstract

The drive of Alfvén Eigenmodes (AEs) by DT-fusion alphas and their resulting transport could greatly impact the success of future burning plasma tokamaks. However, despite the fact that much about AE stability has been explored, open questions remain, for example, of the exact stability threshold conditions for ITER or other burning plasma experiments, like SPARC. In JET, eight in-vessel antennas actively excite stable AEs, and their eigenfrequencies, toroidal mode numbers, and net damping rates are assessed. Thousands of AE stability measurements have been collected by the Alfvén Eigenmode Active Diagnostic (AEAD) in hundreds of JET plasmas during the recent Hydrogen, Deuterium, Tritium, DT, and Helium campaigns. Such an AE stability database, spanning all four ion species, is presented for the first time. In general, damping is observed to decrease with increasing Hydrogenic mass, but increase for Helium, a trend consistent with radiative damping as the dominant damping mechanism. In addition, modeling validation is achieved via the novel simultaneous measurements of stable and destabilized AEs in both D and DT plasmas. In the former, hybrid kinetic-MHD codes MEGA and NOVA-K demonstrate impressive agreement with both growth and damping rates for $n = 2 - 6$ Toroidicity-induced AEs. In DT, NOVA-K finds similar agreement, but for a stable, edge-localized $n = 3$ Ellipticity-induced AE. These specific data points, as well as the entire database, are incredibly important for confident predictions of AE stability in both pre-fusion-power (H/He) and D/T operations in future devices. In particular, if radiative damping plays significant role in their overall stability, some AEs could be more easily destabilized in D/T plasmas than their H/He counterparts, even before considering alpha particle drive.

[1] See the author list of "Overview of T and D-T results in JET with ITER-like wall" by C.F. Maggi *et al.* to be published in *Nuclear Fusion Special Issue: Overview and Summary Papers from the 29th Fusion Energy Conference* (London, UK, 16-21 October 2023)

1. JET'S ALFVÉN EIGENMODE ACTIVE DIAGNOSTIC

The Alfvén Eigenmode Active Diagnostic (AEAD) actively probes *stable* AEs in the JET tokamak [1, 2]. Two toroidal arrays of antennas (four each, eight total) are positioned just below the midplane on the outboard wall inside vacuum vessel. Each 18-turn antenna can be independently powered with currents up to ~ 10 A, and the antennas' phasing can be tuned so that the resulting perturbation has a dominant toroidal mode number $|n| < 20$. Four sets of filters, with different frequency bands, allow the antennas' frequency to span the range $f = 25 - 330$ kHz, with Toriodicity-induced AEs (TAEs) typically in the range $f \approx 100 - 300$ kHz in JET plasmas.

As the AEAD frequency scans through the resonant frequency of a stable AE, the plasma responds like a resonant cavity or a driven, damped harmonic oscillator. Arrays of high frequency magnetic probes measure this response, from which the eigenfrequency $\omega_0 = 2\pi f_0$, mode number n, and net damping rate $\gamma < 0$ can be inferred. Many damping mechanisms can contribute to the total damping rate: continuum, radiative, collisional, Landau damping, and more. The mode can also experience drive, like that from fast ions, which pushes it toward instability ($\gamma > 0$). Thus, the alpha drive of AEs could be assessed directly by comparing two measurements in D and DT plasmas, assuming all other relevant plasma parameters are similar.

An unambiguous measurement of alpha drive of a stable AE has not yet been achieved by the AEAD, although attempts will be made during the 2023 JET DT campaign. Nevertheless, this system has successfully resonated with thousands of AEs in hundreds of JET plasma discharges across multiple recent campaigns with many novel observations. In this paper, database trends for various fuel ion species are explored in Section 2, while Section 3 validates AE stability models using *simultaneous* measurements of destabilized and stabilized AEs. A summary is given in Section 4.

2. DATABASE ANALYSES ACROSS H, D, T, DT, AND HE PLASMAS

2.1. Trends with ion mass number

From 2019 through 2022, several single-species campaigns were carried out on JET to study isotope effects and prepare for the 2021 DT campaign [3]. Across the Hydrogen, Deuterium, Tritium, and Helium campaigns, a database of AE stability measurements was assembled from hundreds of plasmas and with thousands of data points collected. To the authors' knowledge, this work is the first to explore AE stability across all four species of thermal ions, i.e. mass numbers $A = 1 - 4$. Of course, other studies have investigated a subset of species and AEs: for example, TAEs in H, D, and T [4] as well as H, D, and He plasmas [5] in JET; beta-induced AEs (BAEs) in H and D plasmas in DIII-D [6]; and various *fast* ion species in multiple tokamaks.

Because all five JET campaigns did not necessarily explore the same "plasma parameter space," several filters are applied to the data set in order to consider a common subset: plasma currents $I_P = 1 - 3$ MA; toroidal magnetic field strengths $B_T = 1 - 2.5$ T; and minimal external heating powers ($P < 1$ MW) from Neutral Beam Injection (NBI) and Ion Cyclotron Resonance Heating (ICRH) to minimize any contribution from fast ion drive and isolate the effects of damping. Uncertainties in the normalized damping rate and resonant frequency are also restricted to $|\Delta(\gamma/\omega_0)| < 1\%$ and $|\Delta f_0| < 1$ kHz, respectively.

Net damping rates, normalized to the resonant frequency, for all filtered data are shown in Fig. 1a as a function of the effective mass number $A = \sum_i A_i n_i / \sum_i n_i$, with n_i the ion density, assessed from edge spectroscopy. The data are well clustered around the expected mass numbers for each species and campaign. The slight skew toward lower A values for D, T, and He plasmas is likely due to small fractions of H in some plasmas. For DT plasmas, the ratio D/T was scanned more deliberately, seen as several distinct groupings. A trend of decreasing damping rate with mass number is observed in the data for the Hydrogenic species ($A = 1 - 3$), approximately following an inverse relationship ($-\gamma/\omega_0 \propto 1/A$), dashed in Fig. 1a). However, the trend fails for He which displays higher damping rates than T data.

This result is perhaps clearer in the distributions of data shown in Fig. 1b, where the median, 25% and 75% quartiles, and 5% and 95% quantiles are indicated for each campaign's data set. The median damping rate decreases with A from H to D to T plasmas, but increases for He plasmas. There are clear differences in the distributions of H vs D plasmas and T vs He plasmas.[2] The distributions of D, DT, and T data are much more alike; however, all quantiles are still lower for T than D data, with DT values falling somewhere in between. This confirms the inverse relationship of γ/ω_0 and A for the Hydrogenic plasmas. Interestingly, the distributions for D and He plasmas are quite dissimilar, even though they have the same charge-to-mass ratio Z/A and therefore similar Alfvén dynamics.

[2] Note that the spread in each distribution could be due to variety of damping mechanisms: continuum, electron and ion Landau damping, and more; further investigations are left for future work.

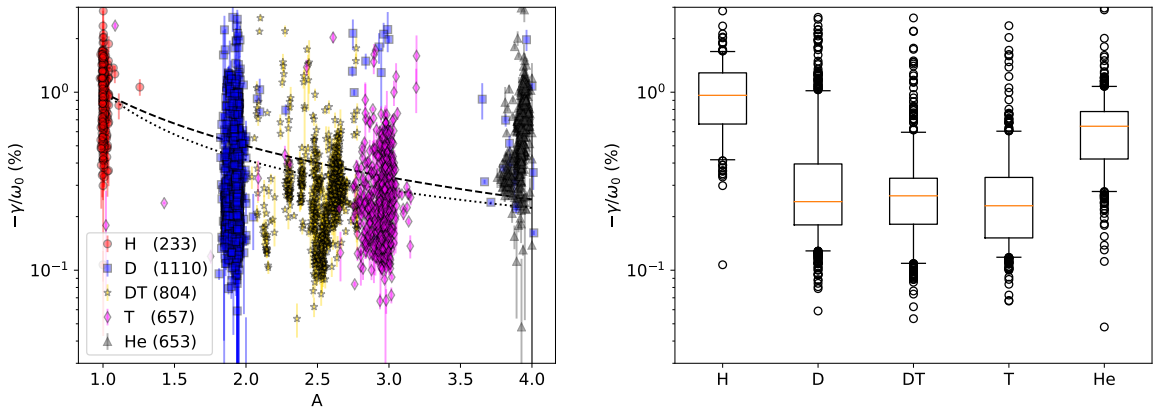

(a) *(b)*

FIG. 1. (a) Normalized damping rate $-\gamma/\omega_0$ vs mass number A for H (red circles), D (blue squares), DT (gold stars), T (magenta diamonds), and He (black triangles) plasmas with the number of data points in parentheses. Lines $-\gamma/\omega_0 \propto 1/A$ and $\exp(constant/\sqrt{A})$ are dashed and dotted, respectively. (b) Box plots for the same data: the yellow solid line indicates the median, box the first and third quartiles, whiskers the 5% and 95% quantiles, and circles the outliers.

This trend of decreasing AE damping rate with ion mass has been reported before. In [4], AE stability measurements across $A = 1 - 2.8$ were analyzed. Analytically, electron Landau damping was expected to scale as $-\gamma/\omega_0 \propto \sqrt{A}$, disagreeing with experiment; however, gyrokinetic simulations matched the empirical finding of an inverse relationship, $-\gamma/\omega_0 \propto 1/A$, which was ultimately attributed to radiative damping via mode conversion to Kinetic Alfvén Waves.

The study in [5] complemented the previous analysis with data ranging $A = 1.7 - 3.95$. Similar decreasing trends were identified, although toroidal mode number discrimination was able to capture an increasing trend $-\gamma/\omega_0 \propto A$. Importantly, the authors used an analytic expression for radiative damping in the form $-\gamma/\omega_0 \propto \exp(G/\lambda)$ [7]. Here, G is a prefactor depending mostly on the mode location in the Alfvén continuum, and $\lambda \propto q(\mathrm{d}q/\mathrm{d}r)\rho_i$ is a "non-ideal" parameter depending on the safety factor profile q, magnetic shear, and finite ion Larmor radius ρ_i. From this, the relationship $-\gamma/\omega_0 \propto \exp(G'/\sqrt{A})$ was proposed in [5], which also matches the Hydrogenic data well in Fig. 1a (dotted line).

Yet this could also explain the divergence of He data from the decreasing trend as the Larmor radius depends on both mass and charge: $\rho_i \sim m_i v_{th,i}/qB \sim \sqrt{m_i T_i}/qB \propto Z/\sqrt{A}$. Thus, a more appropriate expression for radiative damping could be $-\gamma/\omega_0 \propto \exp(G'\,Z/\sqrt{A})$, with damping larger for He plasmas than D and T plasmas (since $2/\sqrt{4} = 1 > 1/\sqrt{2}$ and $1/\sqrt{3}$). However, this formula would imply that H and He data should have the *same* damping (since $1/\sqrt{1} = 2/\sqrt{4}$), which is not reflected in Fig. 1. Simulations with MHD codes MISHKA [8] and CASTOR [9] are underway to better evaluate dependencies on n, Z, A and the contributions of various damping mechanisms, which might explain this discrepancy. Nevertheless, these raw damping rate data are important for future devices since, all else constant, AEs may be better stabilized in pre-fusion-power operations with H/He plasmas and thus more readily destabilized in D/T.

2.2. Trends with other plasma parameters

Dependencies of stable AE damping rates on other plasma parameters can also be explored for each campaign via the database. Table 1 gives Pearson correlation coefficients r_W, weighted by inverse variance, of the normalized damping rate with the edge safety factor q_{95} and edge magnetic shear s_{95}, another formulation of the non-ideal parameter $\lambda' = q_{95}s_{95}\sqrt{T_{e0}}/B_0$ [10] (with T_{e0} and B_0 the on-axis electron temperature and magnetic field strength, respectively), and external heating powers from NBI and ICRH, across the different campaigns. Note that the aforementioned data filter is not used here in order to see trends including *all* data within each campaign.

Strong correlations ($r_\mathrm{W} > 0.5$) are observed with q_{95}, s_{95}, and λ' for the Hydrogenic plasmas. This indicates that continuum and especially radiative damping are major contributions to AE stability for much of the data collected in these campaigns. In contrast, the He campaign shows a moderate correlation with q_{95} and λ', but essentially no correlation with s_{95};[3]thus, while continuum damping may still play a role, radiative damping

[3]The range of s_{95} data is narrower for He compared to other campaigns, which could contribute to this vanishingly small correlation.

TABLE 1. WEIGHTED LINEAR CORRELATION WITH NORMALIZED DAMPING RATE

$r_{\mathrm{W}}(-\gamma/\omega_0,\cdot)$	q_{95}	s_{95}	λ'	P_{NBI}	P_{ICRH}
H	0.79	0.65	0.76	N/A	-0.18
D [11]	0.54	0.57	0.69	0.28	-0.09
T	0.71	0.70	0.74	-0.11	-0.04
DT	0.46	0.61	0.65	0.10	0.14
He	0.39	$\sim$0.00	0.31	-0.20	0.07

appears to be reduced. This is consistent with the trend observed in Fig. 1 and could explain why the median damping rate is higher for H than He plasmas.

Weak correlations ($r_{\mathrm{W}} < 0.3$) are observed with NBI and ICRH powers,[4] suggesting that they contribute minimally to the damping or drive of the stable AEs. This is likely due to the AEAD's improved coupling with the plasma edge [12], where modes have less interaction with core-localized NBI or ICRH fast ions. However, the AEAD *can* measure stable AEs with significant fast ion drive, as explored in the next section.

3. SIMULTANEOUS MEASUREMENTS OF STABILIZED AND DESTABILIZED AES

Reference [13] reported on a novel observation of stabilized and destabilized TAEs measured *simultaneously* in JET Deuterium plasma JPN 94700. During an experiment with three-ion-heating scenario D-(DNBI)-He3 [14], $n = 3-5$ TAEs were clearly destabilized while an $n = 6$ TAE, with damping rate $-\gamma/\omega_0 \approx 2\% \pm 1\%$, was resonantly excited by the AEAD. The simultaneity was crucial in providing multiple data points to validate simulations of the plasma and AE stability at a single point in time. Hybrid kinetic-MHD modeling with both the linear code NOVA-K [15, 16, 17] and nonlinear code MEGA [18] successfully identified the various modes, their toroidal mode numbers and eigenfrequencies. Impressively, both codes matched the measured damping rate of the $n = 6$ TAE within experimental uncertainties, and NOVA-K found radiative damping ($\gamma/\omega_0 \approx -4.8\%$) to dominate the drive from ICRH ($\gamma/\omega_0 \approx +2.3\%$). However, only MEGA could reproduce the stability of all unstable ($n = 3-5$) and stable ($n = 2, 6$) modes.

During the 2021 JET DT campaign, another simultaneous measurement of unstable and stable AEs was made in JPN 99896 [19, 20], this time with $\sim$1% H-minority ICRH. Figure 2a shows the time evolution of plasma parameters for this pulse (50%/50% DT); steady-state values are the on-axis magnetic field strength $B_0 \approx 2.8$ T, plasma current $I_P \approx 1.9$ MA, central electron density $n_{\mathrm{e0}} \approx 4 \times 10^{19}$ m^{-3} and temperature $T_{\mathrm{e0}} \approx 6$ keV. External heating powers are $P_{\mathrm{NBI}} \approx 3-7$ MW from $t \approx 6-11$ s (D-NBI before and T-NBI after $t \approx 9$ s) and $P_{\mathrm{ICRH}} \approx 4.5$ MW from $t \approx 7-12$ s. Profiles at a single time of interest, $t = 11.2$ s, are shown in Fig. 2b: safety factor q from pressure-constrained EFIT, n_{e} and T_{e} from Thomson Scattering, and rotation frequency f_{rot} from charge exchange spectroscopy.

During ICRH heating (shaded in Fig. 2a), $n = 1-6$ TAEs are destabilized; these are seen in the spectrogram of Fig. 3a, which includes a toroidal mode number analysis. The number and frequencies of these modes are interesting: Some are closely spaced in frequency, as might be expected from plasma rotation, i.e. $\Delta f \sim f_{\mathrm{rot}} \sim 1$ kHz, yet others have spacing $\Delta f \sim 10$ kHz. Multiple TAEs with the same n also appear. From [19], this is attributed to the nonlinear interplay between some TAEs and Neoclassical Tearing Modes also present in the discharge. However, further analysis of these *destabilized* TAEs is outside the scope of this paper.

The AEAD was scanning in frequency from $f = 125-250$ kHz during this pulse, seen as the triangular waveform in Fig. 3a. A stable AE was tracked in real time from $t \approx 11-11.5$ s and $f \approx 230-250$ kHz, with a dominant toroidal mode number $n \approx 3$ indicated from the mode analysis. During this period, the injected NBI power was zero, which often improves stable AE detection (from higher signal to noise) [11]. Note how the stable AE frequency increases at approximately the same rate as the other destabilized TAEs over the same time interval. This is likely due to the decreasing density (see Fig. 2a) and thus increasing Alfvén speed over that duration.

The individual stable AE resonance measurements are shown in Fig. 3b. Peaks in the magnetics data (summed over all probes) are fit with a transfer function [1, 2] to identify the resonant frequency and damping rate. Unfortunately, some peaks are too close together to get a reliable fit, so some data appear to be missing. Yet the data indicate a marginally stable $n = 3$ AE with normalized damping rate $-\gamma/\omega_0 \approx 0.4\% - 0.5\%$ increasing in frequency from $f_0 \approx 230-250$ kHz.

Modeling with NOVA-K was performed at one time-slice, $t = 11.2$ s, using the profile data in Fig. 2b. Also included were the distribution functions of NBI and ICRH fast ions as well as DT alphas from TRANSP [21, 22, 23] using the NUBEAM [24] and TORIC [25] modules. Toroidal mode numbers $n = 1-6$ were assessed,

[4] No NBI was used during the H campaign.

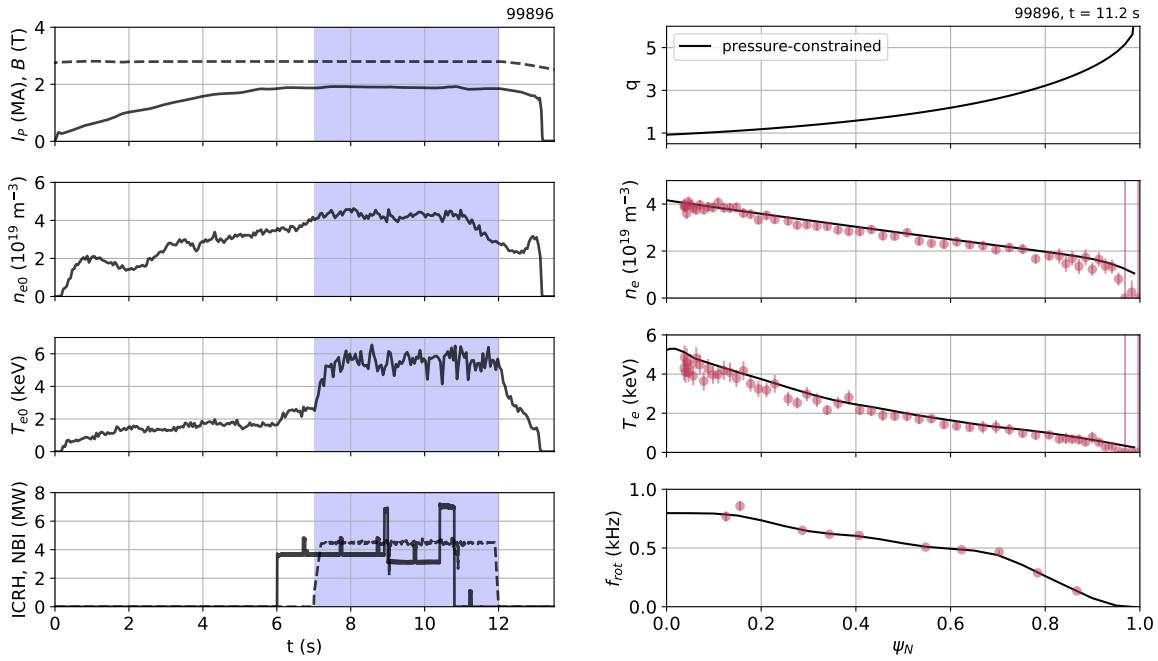

(a) *(b)*

FIG. 2. (a) Plasma parameters for JPN 99896: toroidal magnetic field (dashed), plasma current (solid), central electron density and temperature from Thomson scattering (TS), and heating powers from NBI (solid) and ICRH (dashed). Stable and unstable AEs were measured during the shaded time interval. (b) Profiles at t = 11.2 s: safety factor from pressure-constrained EFIT, electron density and temperature from TS, and rotation frequency from charge exchange. Experimental data are circles with uncertainties as error bars; solid lines are fits to the data; and ψ_N is the normalized poloidal flux.

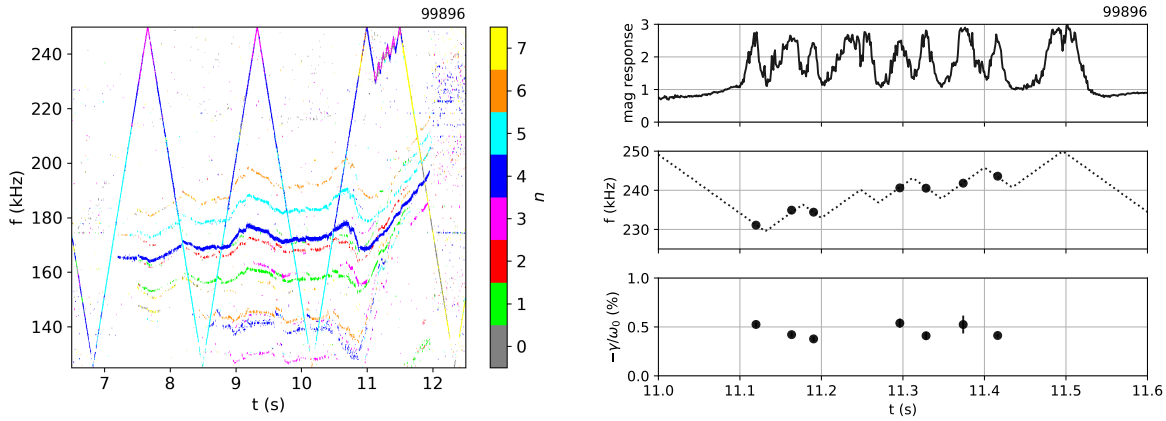

(a) *(b)*

FIG. 3. (a) Fourier decomposition of magnetics data, frequency vs time, with toroidal mode number analysis for JPN 99896. (b) Stable AE resonance measurements: the magnetic response amplitude (summed over all probes), AEAD (dotted) and AE resonant frequencies (circles), and normalized damping rates with uncertainties as error bars.

but only an $n = 3$ edge-localized Ellipticity-induced AE (EAE) was found to match the frequency measured in experiment, $f_0 \approx 235$ kHz. Figure 4 shows the Alfvén continua for $n = 3$, where the $q = 1$ surface is located at $\sqrt{\psi_N} \approx 0.3 - 0.4$ (or $\psi_N \approx 0.1 - 0.15$ in Fig. 2b). The identified mode, at $f_0 = 230$ kHz, lies above the TAE gap, in the edge EAE gap, with dominant poloidal harmonics $m, m + 2 = 5, 7$.

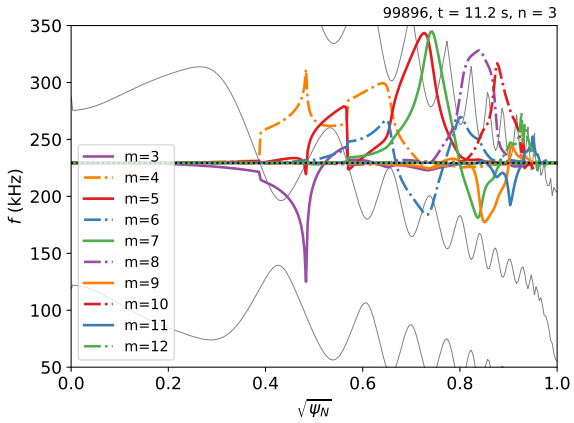

FIG. 4. Alfvén continua (thin lines) and mode structure for poloidal harmonics $m = 3 - 12$ (solid, dot-dashed lines) for the $n = 3$ EAE from NOVA-K, JPN 99896 at $t = 11.2$ s. The lab-frame frequency is indicated by the horizontal dotted line, and ψ_{N} is the normalized poloidal flux.

Individual contributions from various drive and damping mechanisms to the total growth rate ($\gamma/\omega_0 > 0$) are computed by NOVA-K and provided in Table 2. Continuum damping has a small contribution, but large uncertainties, and is evident from the mode-continuum crossings in Fig. 4. Due to the high EAE frequency (compared to the TAEs in Fig. 3a), electron Landau damping dominates over that from D or T ions. Interestingly, NOVA-K finds that both NBI and ICRH fast ions *damp* the mode, likely due to the mode's location closer to the plasma edge. Unfortunately, and likely for the same reason, the alpha drive is effectively zero in this relatively low-power pulse. Nevertheless, the total computed damping rate is $-\gamma/\omega_0 \approx 0.4\% \pm 0.1\%$, which agrees well with that measured in experiment within uncertainties.

TABLE 2. CONTRIBUTIONS TO THE TOTAL GROWTH RATE FOR THE $N = 3$ EAE

Damping/drive mechanism	γ/ω_0 (%)
Continuum	-0.04 ± 0.10
Radiative	$+0.00$
Electron collisional	-0.01
Electron Landau	-0.17 ± 0.01
Deuterium Landau	-0.01
Tritium Landau	-0.01
NBI fast ions	-0.08 ± 0.01
ICRH fast ions	-0.08 ± 0.01
Alphas	$+0.00$
Total	$\mathbf{-0.39 \pm 0.10}$

Although outside the scope of this work, it should be noted that NOVA-K fails to identify any of the destabilized TAEs observed in experiment (see Fig. 3a). Therefore, while NOVA-K is able to accurately assess the AE stability physics in the outer region of the plasma, $\sqrt{\psi_{\mathrm{N}}} > 0.5$, not all is captured in the core. However, these unstable modes are reproduced in the modeling of [19], which includes nonlinear coupling not available in NOVA-K. A complementary follow-up study with MEGA could be pursued in the future.

4. SUMMARY

The recent single-species campaigns at the JET tokamak, leading up to the 2021 DT campaign, have allowed the compilation of a comprehensive database of Alfvén Eigenmode (AE) stability across H, D, T, DT, and He plasmas using the Alfvén Eigenmode Active Diagnostic (AEAD). Stable AE data from this recent He campaign are presented here for the first time, and this work could also be the first to analyze AE stability in plasmas with mass numbers spanning $A = 1 - 4$. As the mass number increased from H to D and DT to T campaigns, the distribution of normalized damping rates was found to shift toward lower values (see Fig. 1). This was consistent with previous isotope effect studies [4, 5] which attributed decreasing trends, e.g. $-\gamma/\omega_0 \propto 1/A$ or $\exp(1/\sqrt{A})$, to significant radiative damping. At first glance, the He data seem to contradict this conclusion as the distribution moves toward

higher damping values; however, further inspection of radiative damping reveals a scaling $-\gamma/\omega_0 \propto \exp(Z/\sqrt{A})$ with the introduction of charge Z through the finite ion Larmor radius, a non-ideal/kinetic effect.

An investigation of correlations within individual campaigns (see Table 1) further supports the dominance of radiative damping in the database. In particular, the damping rate is well correlated with the "non-ideal parameter" [10] associated with radiative damping. Strong correlations are found for Hydrogenic plasmas, whereas the moderate correlation for He plasmas could explain differences in the damping rate distributions of H and He plasmas, which otherwise have the same value of $Z/\sqrt{A}$. Regardless, these data indicate that radiative damping may play less of a role in AE stability for D/T plasmas than H/He plasmas; this could result in AEs being more easily destabilized in D/T discharges, even without alpha drive. Future tokamak operators must take this effect into account when moving from pre-nuclear to nuclear phases.

The 2021 JET DT campaign also allowed a repeat of stable and unstable AEs measured simultaneously [13]. Toroidicity-induced AEs (TAEs) with toroidal mode numbers $n = 1 - 6$ were destabilized during ~ 4 MW of Neutral Beam Injection (NBI) and ~ 4.5 MW of Ion Cyclotron Resonance Heating (ICRH) (see Figs. 2 and 3). The AEAD actively resonated with and tracked in real time an $n = 3$ Ellipticity-induced AE (EAE) with a frequency ($f_0 \approx 235$ kHz) clearly higher than the $n = 3$ TAE ($f \approx 160$ kHz).

NOVA-K modeling [15, 16, 17] confirmed the eigenmode as an edge-localized $n = 3$ EAE (see Fig. 4), with such a mode often readily excited by the AEAD because of its closer proximity to the antennas. NOVA-K also matched the measured frequency and normalized damping rate $-\gamma/\omega_0 \approx 0.3 - 0.5\%$ (see Table 2), although unfortunately with no drive from NBI, ICRH, or DT alphas. While edge modes are perhaps less likely to be driven unstable by core-localized fast ion populations, the (oftentimes) spatially broader alpha population could destabilize them, as found in recent simulations [26] and experiments [27]. Moreover, global and edge modes could lead to transport of energetic particles all the way to the plasma edge, thereby degrading confinement. Thus, the validation of these simulations via experimental measurements of f_0, γ, and n from both core and edge-localized AEs gives confidence in extrapolations to future burning plasmas and fusion power plants.

ACKNOWLEDGEMENTS

Many thanks to the JET ICRH team for their experimental support. This work is supported by US DOE grants DE-SC0014264, DE-AC02-09CH11466, DE-SC0020412, DE-SC0020337, and Brazilian agency FAPESP Project 2011/50773-0. This research used resources of the National Energy Research Scientific Computing Center, a US DOE Office of Science User Facility operated under Contract No. DE-AC02-05CH11231 using NERSC award FES-ERCAP20598. This work has been carried out within the framework of the EUROfusion Consortium, via the Euratom Research and Training Programme (Grant Agreement No 101052200 — EUROfusion) and funded by the Swiss State Secretariat for Education, Research and Innovation (SERI). Views and opinions expressed are however those of the author(s) only and do not necessarily reflect those of the European Union, the European Commission, or SERI. Neither the European Union nor the European Commission nor SERI can be held responsible for them.

REFERENCES

[1] A. Fasoli, D. Borba, G. Bosia, D. J. Campbell, J. A. Dobbing, C. Gormezano, J. Jacquinot, P. Lavanchy, J. B. Lister, P. Marmillod, J. M. Moret, A. Santagiustina, and S. Sharapov. Direct measurement of the damping of toroidicity-induced Alfvén eigenmodes. *Physical Review Letters*, 75(4):645–648, 1995.

[2] P. Puglia, W. Pires de Sa, P. Blanchard, S. Dorling, S. Dowson, A. Fasoli, J. Figueiredo, R. Galvão, M. Graham, G. Jones, C. Perez von Thun, M. Porkolab, L. Ruchko, D. Testa, P. Woskov, M.A. Albarracin-Manrique, and JET Contributors. The upgraded JET toroidal Alfvén eigenmode diagnostic system. *Nuclear Fusion*, 56(11):112020, 2016.

[3] J. Mailloux et al. Overview of JET results for optimising ITER operation. *Nuclear Fusion*, 62(4):042026, 2022.

[4] A. Fasoli, A. Jaun, and D. Testa. Isotope mass scaling of AE damping rates in the JET tokamak plasmas. *Physics Letters, Section A: General, Atomic and Solid State Physics*, 265(4):288–293, 2000.

[5] D. Testa, T. Panis, P. Blanchard, A. Fasoli, and JET-EFDA Contributors. Plasma isotopic effect on the damping rate of toroidal Alfvén eigenmodes with intermediate toroidal mode numbers. *Nuclear Fusion*, 52:094006, 2012.

[6] W.W. Heidbrink, G.J. Choi, M.A. Van Zeeland, M.E. Austin, G.H. Degrandchamp, D.A. Spong, A. Bierwage, N.A. Crocker, X.D. Du, P. Lauber, Z. Lin, and G.R. McKee. Isotope dependence of beta-induced Alfvén eigenmode (BAE) and low frequency mode (LFM) stability in DIII-D. *Nuclear Fusion*, 61(10):106021, 2021.

[7] J.W. Connor, R.O. Dendy, R.J. Hastie, D. Borba, G. Huysmans, W. Kerner, and S. Sharapov. Non-ideal effects on toroidal alfvén eigenmode stability. In *Europhysics Conference Abstracts*, volume 18, pages 616–619, 1994.

[8] A. B. Mikhailovskii, G. T. A. Huysmans, W. O. K. Kerner, and S. E. Sharapov. Optimization of computational MHD normal-mode analysis for tokamaks. *Plasma Physics Reports*, 23(10):844–857, 1997.

[9] G. T. A. Huysmans, S. E. Sharapov, A. B. Mikhailovskii, and W. Kerner. Modeling of diamagnetic stabilization of ideal magnetohydrodynamic instabilities associated with the transport barrier. *Physics of Plasmas*, 8(10):4292–4305, 2001.

[10] W. W. Heidbrink. Basic physics of Alfvén instabilities driven by energetic particles in toroidally confined plasmas. *Physics of Plasmas*, 15(5):055501, 2008.

[11] R.A. Tinguely, N. Fil, P.G. Puglia, S. Dowson, M. Porkolab, V. Guillemot, M. Podestà, M. Baruzzo, R. Dumont, A. Fasoli, M. Fitzgerald, Ye.O. Kazakov, M.F.F. Nave, M. Nocente, J. Ongena, S.E. Sharapov, Ž. Štancar, and JET Contributors. A novel measurement of marginal Alfvén eigenmode stability during high power auxiliary heating in JET. *Nuclear Fusion*, 62(7):076001, 2022.

[12] R.A. Tinguely, P.G. Puglia, N. Fil, S. Dowson, M. Porkolab, A. Dvornova, A. Fasoli, M. Fitzgerald, V. Guillemot, G.T.A. Huysmans, M. Maslov, S. Sharapov, and D. Testa. Experimental studies of plasma-antenna coupling with the JET Alfvén Eigenmode Active Diagnostic. *Nuclear Fusion*, 61:26003–26017, 2021.

[13] R.A. Tinguely, J. Gonzalez-Martin, P.G. Puglia, N. Fil, S. Dowson, M. Porkolab, I. Kumar, M. Podestà, M. Baruzzo, A. Fasoli, Ye.O. Kazakov, M.F.F. Nave, M. Nocente, J. Ongena, Ž. Štancar, and JET Contributors. Simultaneous measurements of unstable and stable Alfvén eigenmodes in JET. *Nuclear Fusion*, 62(11):112008, 2022.

[14] Ye.O. Kazakov, M. Nocente, M.J. Mantsinen, J. Ongena, Y. Baranov, T. Craciunescu, M. Dreval, R. Dumont, J. Eriksson, J. Garcia, et al. Plasma heating and generation of energetic D ions with the 3-ion ICRF+ NBI scenario in mixed HD plasmas at JET-ILW. *Nuclear Fusion*, 60(11):112013, 2020.

[15] C.Z. Cheng. Kinetic extensions of magnetohydrodynamics for axisymmetric toroidal plasmas. *Physics Reports*, 211(1):1–51, 1992.

[16] G.Y. Fu and C.Z. Cheng. Excitation of high-n toroidicity-induced shear Alfvén eigenmodes by energetic particles and fusion alpha particles in tokamaks. *Physics of Fluids B: Plasma Physics*, 4(11):3722–3734, 1992.

[17] N.N. Gorelenkov, C.Z. Cheng, and G.Y. Fu. Fast particle finite orbit width and Larmor radius effects on low-n toroidicity induced Alfvén eigenmode excitation. *Physics of Plasmas*, 6(7):2802–2807, 1999.

[18] Y. Todo and T. Sato. Linear and nonlinear particle-magnetohydrodynamic simulations of the toroidal Alfvén eigenmode. *Physics of Plasmas*, 5:1321–1327, 1998.

[19] J. Garcia et al. Stable Deuterium-Tritium burning plasmas with improved confinement in the presence of energetic-ion instabilities. 2023. In progress.

[20] J. Garcia et al. Overview of alpha particle and fast ion studies in JET DTE2 plasmas. To be published in *Nuclear Fusion Special Issue: Overview and Summary Papers from the 29th Fusion Energy Conference* (London, UK, 16-21 October 2023).

[21] J. Breslau, M. Gorelenkova, F. Poli, J. Sachdev, and X. Yuan. TRANSP. [Computer Software] `https://doi.org/10.11578/dc.20180627.4`, jun 2018.

[22] R.J. Hawryluk. An empirical approach to tokamak transport. In Coppi et al, editor, *Physics Close to Thermonuclear Conditions, Ed. B*, volume 19. Brussels: Commission of the European Communities, Brussels, 1980.

[23] J.P.H.E. Ongena, I. Voitsekhovitch, M. Evrard, and D. McCune. Numerical transport codes. *Fusion Science and Technology*, 61(2T):180–189, 2012.

[24] A. Pankin, D. McCune, R. Andre, G. Bateman, and A. Kritz. The tokamak Monte Carlo fast ion module NUBEAM in the National Transport Code Collaboration library. *Computer Physics Communications*, 159(3):157–184, 2004.

[25] M. Brambilla. Numerical simulation of ion cyclotron waves in tokamak plasmas. *Plasma Physics and Controlled Fusion*, 41(1):1–34, jan 1999.

[26] M. Fitzgerald, S.E. Sharapov, P. Siren, E. Tholerus, M. Dreval, G. Szepesi, P. Vallejos, T. Johnson, N. Fil, J. Ferreira, P. Rodrigues, A. Figueiredo, D. Borba, R. Coelho, F. Nabais, J. Mailloux, H.J.C. Oliver, C. Di Troia, F. Napoli, Ž. Štancar, R. Dumont, D. Keeling, and JET Contributors. Toroidal Alfvén eigenmode stability in JET internal transport barrier afterglow experiments. *Nuclear Fusion*, 62(10):106001, 2022.

[27] M. Fitzgerald et al. Stability analysis of alpha driven toroidal Alfvén eigenmodes observed in JET deuterium-tritium internal transport barrier plasmas. *Nuclear Fusion*, 2023. Accepted for publication.